INTERNATIONAL JOURNAL FOR NUMERICAL METHODS IN FLUIDS
Int. J. Numer. Meth. Fluids 2002; **40**:723–733 (DOI: 10.1002/fld.373)

Large-scale structures at various stages of separated boundary layer transition

Zhiyin Yang*,†

Department of Aeronautical and Automotive Engineering, Loughborough University, Loughborough LE11 3TU, U.K.

SUMMARY

Large-eddy simulation is employed to investigate separated boundary layer transition induced by a change of curvature of the surface. The geometry is a flat plate with a semi-circular leading edge. The Reynolds number based on the uniform inlet velocity and the leading edge diameter is 3450. The simulated mean and turbulence quantities compare well with the available experimental data. The LES data have been comprehensively analysed to elucidate the transition process leading to breakdown to turbulence. Large-scale structures have been observed at various stage of the transition process. Understanding the formation of these large-scale structures, their evolution and eventual break-up into smaller structures may help to shed light on the transition mechanism. Copyright © 2002 John Wiley & Sons, Ltd.

KEY WORDS: large-eddy simulation; transition; large-scale structures

1. INTRODUCTION

The presence of large-scale organized motions in turbulent shear flows was first suggested by Townsend [1] and numerous studies have revealed aspects of the structure of the organized motion in a wide variety of flows over the past several decades. Such organized motions are present in the early experiment of Corrsin [2] in free turbulent flows. Generally speaking, we call these large-scale organized motions *coherent structures* and many transitional and turbulent flows (if not all) contain them. A brief history of coherent structures is given by Hussain [3] and more information on research in this area can also be found in two review articles by Cantwell [4] and Robinson [5]. A more recent overview on this topic can be found in the monographs by Holmes *et al.* [6].

The topology and range of scales of coherent structures changes widely from flow to flow. For example counter-rotating vortices in wake flows and streaks, hairpin vortices in turbulent boundary layer. A wide range of investigations have been carried out to try to have a better understanding of coherent structures and their dynamical roles in turbulence. Paschereit *et al.*

* Correspondence to: Z. Yang, Department of Aeronautical and Automotive Engineering, Loughborough University, Loughborough LE11 3TU, U.K.
† E-mail: z.yang@lboro.ac.uk

Received June 2001
Revised March 2002

[7] carried out studies of large structures in swirling flows and their role in acoustic combustion control. Jeong *et al.* [8] used a conditional sampling scheme to educe coherent structures near the wall in a numerically simulated turbulent channel flow. Nickels and Marusic [9] developed a different approach to the interpretation of spectra. They compared the experimental spectra with the spectra produced by random arrays of simple vortex structures in an effort to understand the structures of the flows. Their aim is to examine to what extent the experimental results are consistent with an array of simple coherent structures. The coherent structure in the similarity region of a turbulent planar jet is examined experimentally by Gordeyev and Thomas [10] using the proper orthogonal decomposition (POD) technique. Chainais *et al.* [11] studied the relationship between intermittency and coherent structures in a swirling flow by doing a wavelet analysis of the pressure and velocity signals, conditioned to the list of pressure drops.

The discovery of large-scale coherent structures has generated new excitement in turbulent research and changed the classical view that turbulent flows are random fluid motions in a state of total chaos. It is quite exciting because the time evolution of a deterministic structure might be mathematically tractable. However, in spite of widespread interest and some intensive research in these structures there is not yet a consensus on the definition and role of coherent structures. Many definitions have been given to coherent structures as reported by Sherif [12]:

(1) Large-scale organized motion.
(2) A pattern that recurs in the flow which does not necessarily have an order to it; its scale and velocity are random. However, its orientation is fixed.
(3) Predominant modes of instability.
(4) Entities that cause transport of momentum or tracers across a finite distance in a non-diffusive way.

Hussain [3] defined that a coherent structure is a connected, large-scale turbulent fluid mass with a phase-correlated vorticity over its spatial extent and introduced a triple decomposition. That is, any instantaneous variable consists of three components: mean component, the coherent component and the incoherent turbulence. However, implicit in this decomposition is that the coherent structure is a perturbation of the time-mean flow while arguably coherent structure is the flow and not a mere perturbation. He then introduced a double decomposition so that the turbulent shear flow consists of coherent and incoherent motions only, and governing equations with triple and double decompositions were derived.

It is also very debatable how important a role coherent structures play dynamically and how to detect it. Flow visualization is the traditional method which shows that there are indeed large coherent fluid motions present. However, it can be misleading. In addition, one cannot learn much directly about the dynamics of coherent structures from flow visualization. Several experimental techniques have been developed for the extraction of the coherent structure from turbulent shear flows and these are reviewed by Bonnet and Delville [13]. Such techniques may be broadly classified as ‘conditional’ or ‘non-conditional’. Conditional techniques involve sampling the flow only during those intervals of time which satisfy some predetermined criterion that is deemed dynamically significant and is related to the presence of the coherent structure to be sought. One drawback of these techniques is a lack of objectivity in the sense that one must have some predetermined idea regarding the structural topology in order to set the sampling criterion. in contrast, a more rigorous method of identification of coherent structures called POD proposed by Lumley [14], is an example of a non-conditional technique

based on the two-point correlation. An advantage of the method is its objectivity and lack of bias. The mathematical background to the POD is the Karhunen–Loeve expansion as described in Loeve [15].

Coherent structure has been widely and intensively investigated but arguably that research toward understanding the topology and dynamics of time-evolving, three-dimensional coherent structures is still in its infancy, and hence there is not any formalism for incorporating coherent structures explicitly into predictive models although a number of efforts have been made to include them in models of turbulence as briefly discussed by Cantwell [16].

The objective of this paper is not to clarify what coherent structure are and how important a role they play dynamically but to show by processing LES data that some large-scale structures associated with various stages of separated boundary layer transition have been observed, and hopefully to shed some light on the transition mechanism by looking at the evolution of these coherent structures.

2. NUMERICAL PROCEDURE

The fully covariant incompressible Navier–Stokes equations in general co-ordinates are discretized on a staggered mesh using finite volume methods. The governing equations can be regarded as 'implicitly filtered' owing to the use of finite volume methods, which is similar to imposing a top hat filter; the local filter width in this case is equivalent to the local grid spacing. The velocity components at the grid points are interpreted as the volume average. Any small-scale (smaller than the control volume) motions are averaged and have to be accounted for by a subgrid-scale model. A dynamic subgrid-scale model in general co-ordinates has been developed and used in the present study. The explicit second order Adams–Bashforth scheme is used for the momentum advancement except for the pressure term. The Poisson equation for pressure is solved using an efficient hybrid Fourier multigrid method with the periodic boundary conditions applied in spanwise dimension. The spatial discretization is second-order central differencing which is widely used in LES owing to its non-dissipative and conservative properties. Details of the mathematical formulation and numerical methods in general co-ordinates used in the present study have been reported elsewhere by Yang and Voke [17].

Figure 1 shows the computational domain and mesh used in the study. The fully general co-ordinate system around this geometry is needed since an orthogonal co-ordinate system has an inconvenient junction between a cylindrical and a Cartesian mesh region just at the critical point where the curved leading edge joins the flat surface. This is the point at which the laminar flow separates and starts to become unstable. Any disturbances in this region, including those with a numerical origin, affect the flow and may lead to erroneous conclusions. A previous simulation by Voke *et al.* [18] used an orthogonal co-ordinate system and suffered from the problems indicated, including rapid and excessive growth of disturbances in the separated shear layer whose origin could be traced to numerical effects. This does not occur in the simulation with fully general curvilinear co-ordinates.

The simulation uses 408 (streamwise, wrapped round the leading edge) by 72 (wall-normal) by 64 (spanwise) meshes. The circular inflow boundary and the lateral boundaries are eight leading-edge diameters ($8d$) distant from the surface, corresponding to a blockage ratio of 16. The spanwise dimension of the domain is $2d$. The inflow velocity is constant, U_0, and

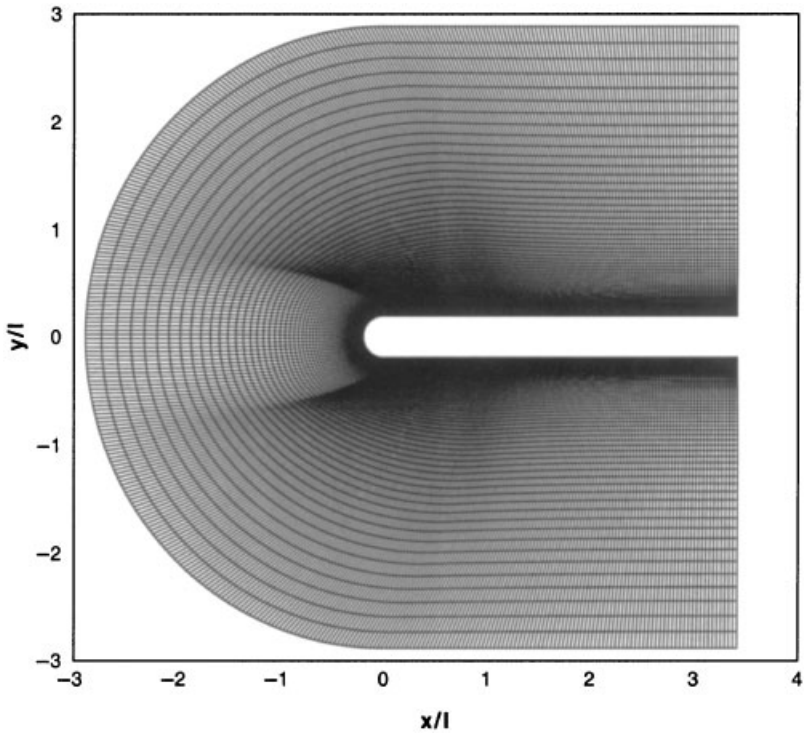

Figure 1. Computational domain and mesh.

aligned with the plate. Random disturbances are imposed just upstream of the separation point to mimic the low turbulence level ($<0.2\%$) in the experiment. The lateral boundaries are free-slip but impermeable. On the outflow boundaries, $9.5d$ downstream of the leading edge, a convective boundary condition based on the mean streamwise velocity.

In terms of wall units based on the shear layer downstream of reattachment at $x/l = 2.5$ (l is the separation bubble length), the streamwise mesh sizes vary from $Dx^+ = 10$ to 30.5, while $Dz^+ = 9$ and at the wall $Dy^+ = 1$ (the distance from the wall to the first cell location of u and w). The time step used in the simulation is $0.005d/U_0$. The averaged subgrid eddy viscosity is about 3.5 times the molecular viscosity as the mesh resolutions are quite fine in most of the important flow region and not far away from what would be recognized as DNS.

The simulation is run for 40 000 time steps to allow the transition and turbulent boundary layer to become established, i.e. the flow has reached a statistically stationary state, and the averaged results presented below are then gathered over a further 60 000 steps with a sample taken every 20 time steps (3000 samples, averaged over the spanwise direction too, corresponding to around 17 flow-through or residence times). Instantaneous flow fields and time trace of velocity components at certain points are also stored during the simulation for subsequent visualization and analysis.

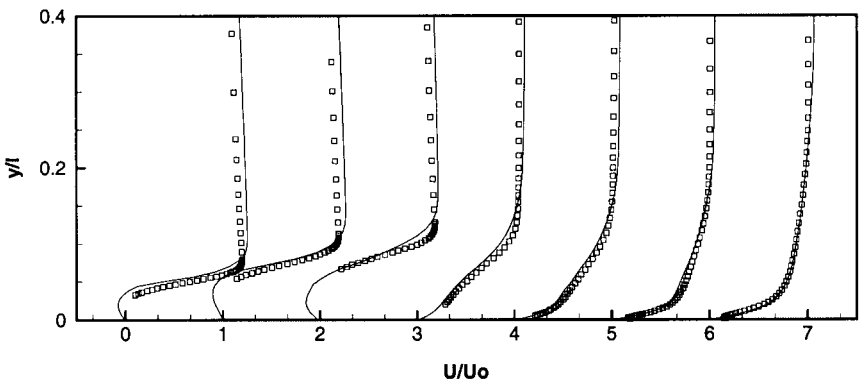

Figure 2. Mean axial velocity at seven streamwise positions measured from the blend point. Left to right, $x/l = 0.22, 0.44, 0.66, 1.09, 1.27, 1.64, 2.55$. Line—LES; Symbols—Exp. data.

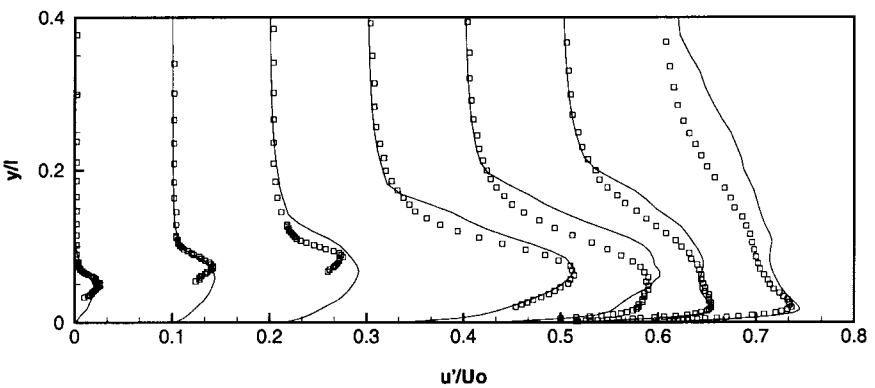

Figure 3. RMS streamwise velocity fluctuation u'; other details as in Figure 2.

3. RESULTS AND DISCUSSION

3.1. Mean variables

The simulated mean and turbulence quantities compare well with the available experimental data [19] as can be seen from Figures 2 and 3 which show the mean and rms fluctuating parts of the streamwise velocity compared with experiment at seven streamwise stations ($x/l = 0.22, 0.44, 0.66, 1.09, 1.27, 1.64, 2.55$). The experimental blockage ratio is lower than that in the simulation. The profiles are plotted as functions of y/l at corresponding values of x/l where l is the mean reattachment length. As can be seen from Figure 2 very good agreement between the experimental data and the simulated results has been obtained for the mean streamwise velocity profiles. Differences in the free stream arise mainly from the difference in blockage ratio. The agreement for the rms fluctuations, as shown in Figure 3, is also good

except that the simulation shows higher peaks of u' occurring closer to the wall at two stations in the bubble, especially at $x/l = 0.66$ where the discrepancy between the peak values is about 25%, but lack of experimental data (taken with a single hot-wire probe) in the near-wall region makes detailed comparisons difficult. After the reattachment the agreement is much better.

3.2. Transition process

The boundary layers develop in the densely meshed regions on either side of the plate, and are fully turbulent well before they reach the two outflow boundaries. The layers on either side of the plate are not symmetric and can be quite different instantaneously, just as they would be in reality. In the earliest stage of the simulation a steady separation bubble appears at the blend point and takes a two-dimensional form similar to that found for a laminar separation bubble at lower Reynolds number. The bubble then grows as the simulation proceeds and at a certain stage the free shear layer formed in the bubble becomes inviscidly unstable owing to small disturbances imposed in the simulation, breaking the separation into two bubbles as the first sign of two-dimensional instability and vortex shedding. The shear layer becomes more unstable and the newly formed bubble breaks up again, with coherent three-dimensional structures appearing.

After several tens of thousands of time steps the flow reaches a statistically stationary state. The transition process can be clearly seen in Figure 4 which shows the instantaneous spanwise vorticity at various times (1000 time steps interval) in the (x, y) plane at an arbitrary z (spanwise) plane as the vorticity at different z planes is similar. In the first half of the bubble a free shear layer develops and 2D spanwise vortices forms; these are inviscidly unstable via the Kelvin–Helmholtz mechanism and any small disturbances present grow downstream with an amplification rate larger than that in the case of viscous instabilities. Further downstream the initial spanwise vortices are distorted severely and roll up, leading to streamwise vorticity formation associated with significant 3D motions, eventually breaking down into relatively smaller turbulent structures after the reattachment point and developing into a turbulent boundary layer rapidly afterwards.

3.3. Large-scale structures

Figure 5 shows contours of streamwise fluctuating velocity at three different heights ($y^+ = 7$, 19, 100) from the wall and the so-called 'streaky structures' are apparent at around and downstream of the mean reattachment line in Figures 5(a) and 5(b) which are very close and fairly close to the wall. The streaky structures are well known in turbulent boundary layer and it is believed that their formation is closely associated with counter-rotating streamwise vortices, which are responsible for ejecting slow-moving fluid from the wall region. This part of the evolution is known as the ejection phase which is associated with the burst of Reynolds stress production, and hence is largely responsible for the maintenance of the turbulence in the boundary layer. Following the Reynolds stress burst it is observed that a gentle downdraft occurs, bringing higher-speed fluid down toward the wall which is called the sweep phase. The streaky structures gradually disappear when moving further away from the wall as shown in Figure 5(c). There is no distinct structures or flow patterns in the first two-thirds of the bubble very close to the wall (a) or slightly away from the wall (b), or far away from the wall (c) apart from the 2D spanwise vortices as shown in Figure 4.

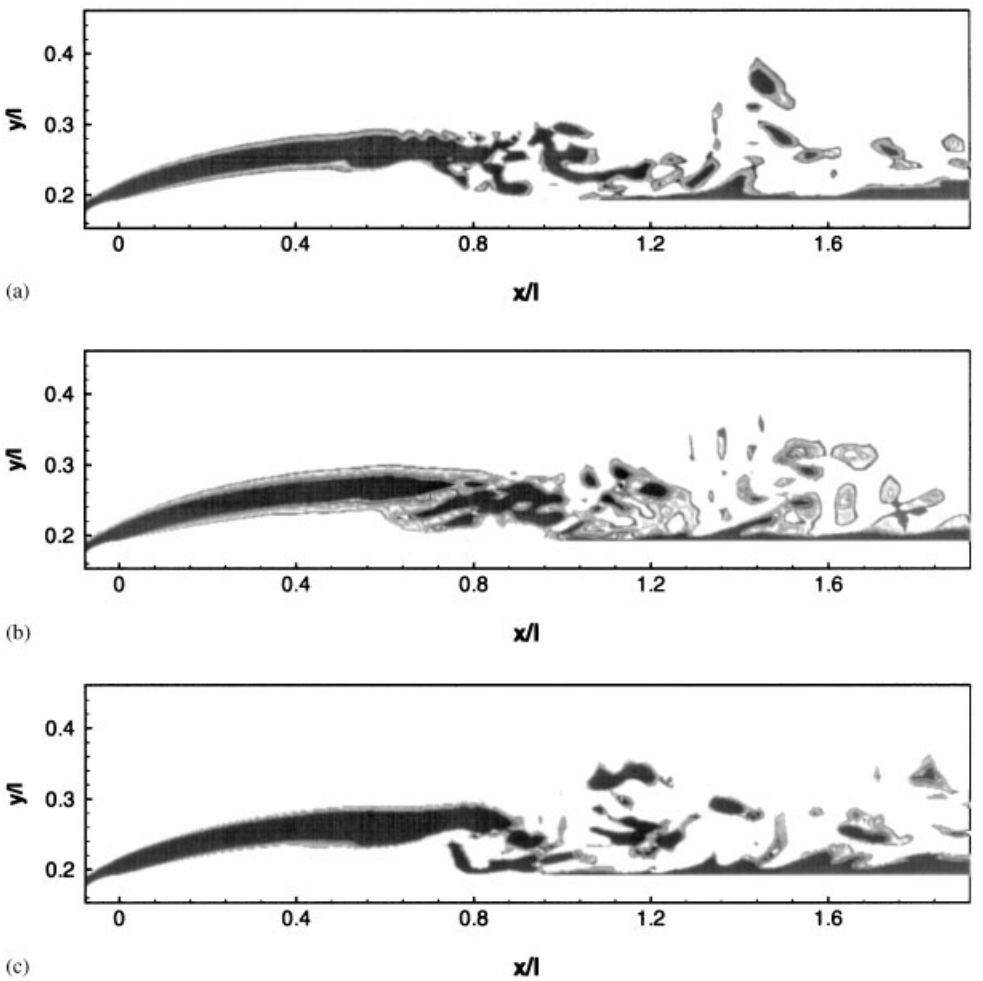

Figure 4. Instantaneous spanwise vorticity in the (x, y) plane.

Figure 6 shows the 3D contours of fluctuating pressure at three different times (1000 time steps interval). It can be seen from Figure 6(a) that 2D vortical structures exist at the early stage of the bubble and then become distorted owing to 3D motion setting in. Hairpin vortices form further downstream around or after the reattachment, as shown in Figures 6(b) and 6(c), and eventually break down to small-scale turbulence structures after the reattachment. The spanwise distance between the ends of the Lambda vortices is about 0.3l (l is the mean separation bubble length), which is roughly the same as the Kelvin–Helmholtz wavelength in the present study. This is worthy of note as it is shown by Roshko [20] that the spanwise distance between the streamwise vortices in the transition region of an initially laminar mixing layer is approximately equal to the Kelvin–Helmholtz spacing. Tafti and Vanka [21] conclude from their numerical study of the unsteady separated flow over a blunt plate held normal to

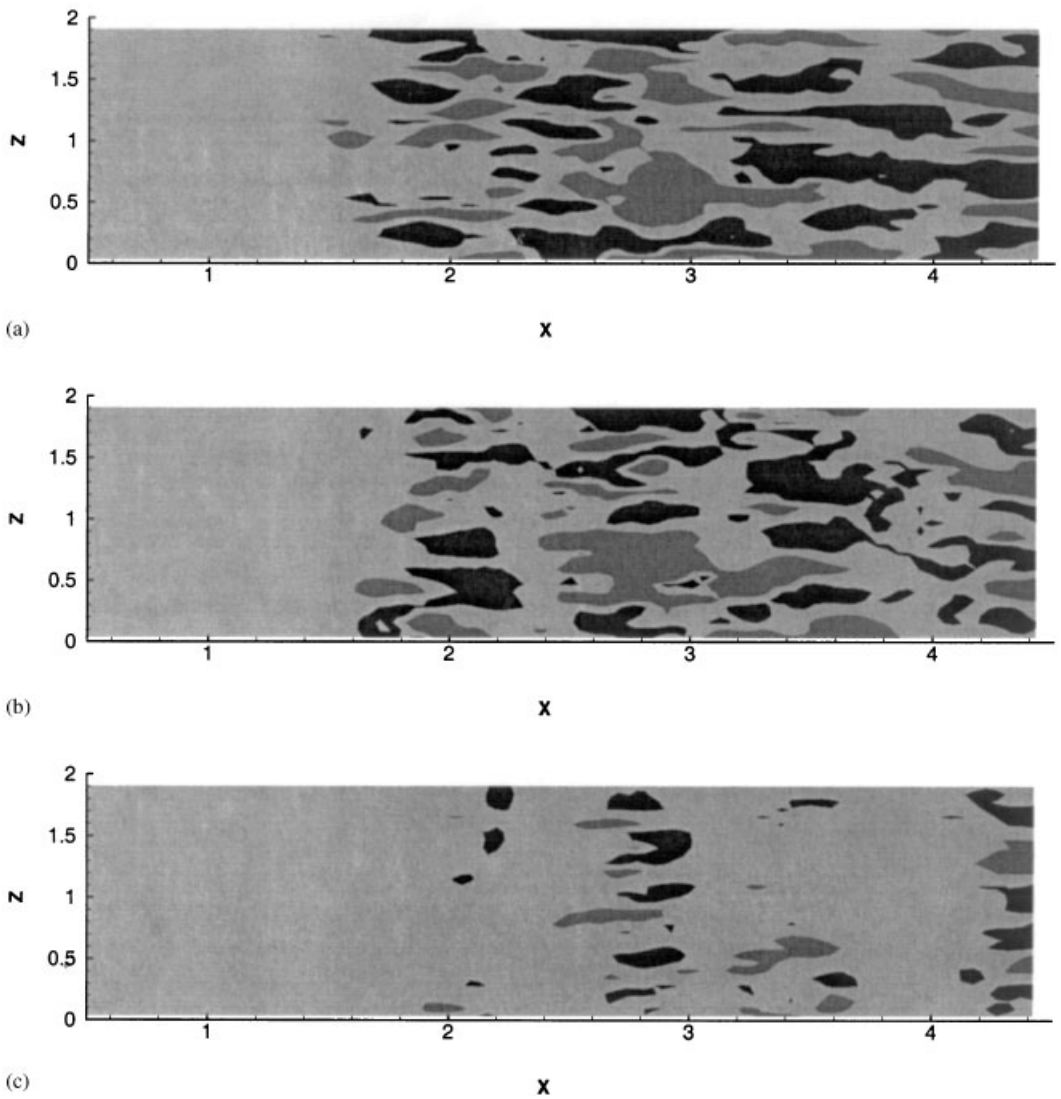

Figure 5. Contours of u' in the (x,z) plane at different heights from the wall.

a uniform stream that the separation bubble is characterized by large coherent structures in the form of spanwise vortices. They are three-dimensional in nature with their approximate spanwise size between 20 and 30% of the mean reattachment length, similar to that observed in the present study.

The hairpin vortical structures identified in the present study also confirm the ideas put forward by Kiya and Sasaki [22] from their experimental study that hairpin vortices exist in the separated flow region. Large-scale structures exist not only in transitional separated flow but also in turbulent separated flow as reported by Na and Moin [23] in their DNS of a

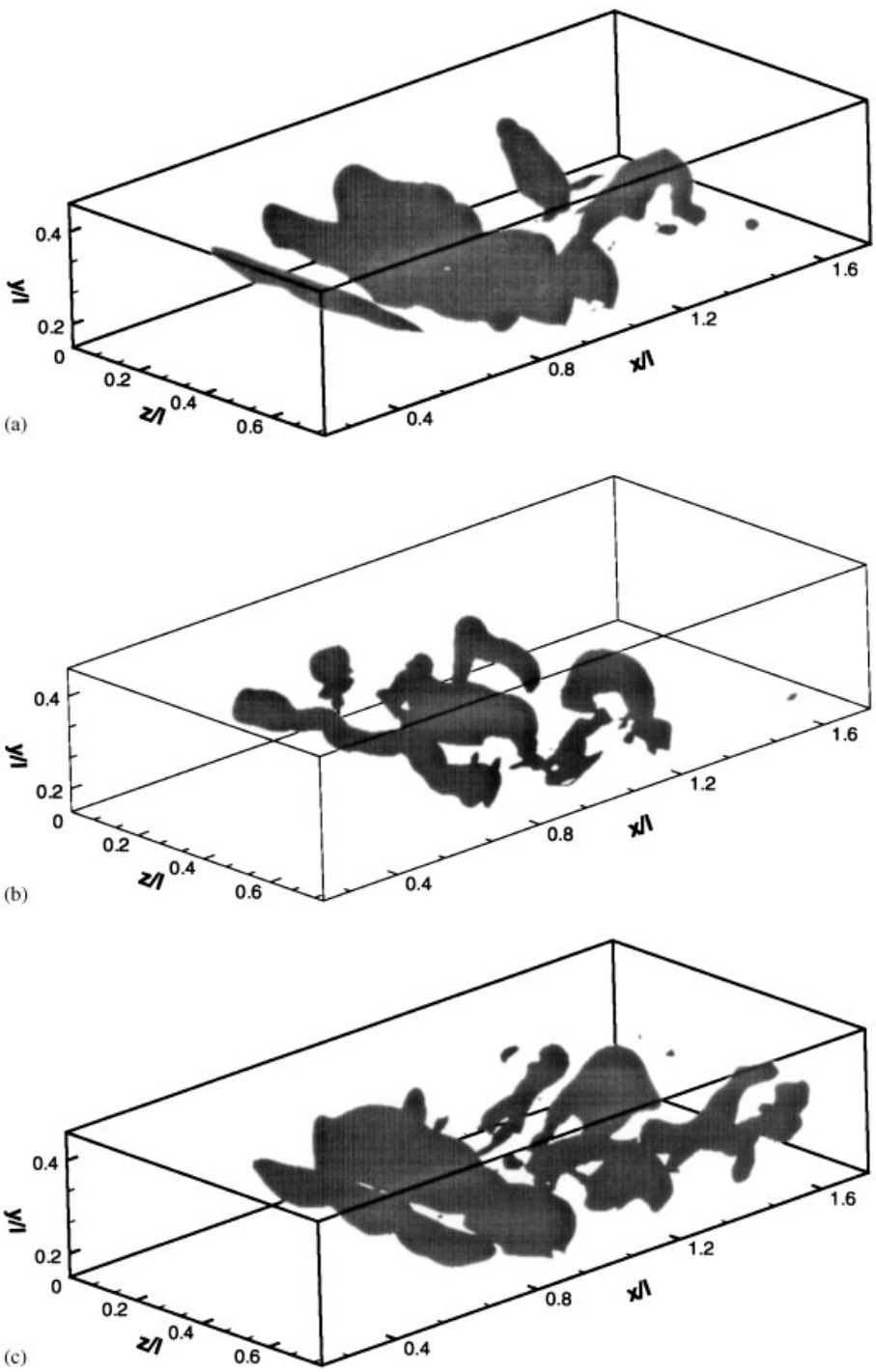

Figure 6. Contours of fluctuating pressure showing vortex cores at three times.

separated turbulent boundary layer on a flat plate due to an adverse pressure gradient. Large-scale structures are clearly identified in the transition process associated with the separation bubble and go through several stages: 2D, distorted 3D, and hairpin vortices, a breakdown stage and eventually turbulence after the reattachment point in the present study.

4. CONCLUSION

It is evident from the simulation that large-scale structures are present at different stages in the separated boundary layer transition. These structures are closely associated with the transition process and play an important role. 2D spanwise vorticity forms at very early stage in the separation bubble. These 2D spanwise vortices get distorted as the free shear layer formed in the separation bubble is inviscidly unstable via the Kelvin–Helmholtz mechanism. 3D motions start to develop initially slowly under any small spanwise disturbance via a secondary instability mechanism associated with the formation of a spanwise peak-valley wave structure. Further downstream the distorted spanwise 2D vortices roll up leading to streamwise vorticity formation. Significant growth of 3D motions occur at about half the mean bubble length with hairpin vortices appearing at this stage, leading eventually to full breakdown to turbulence around the mean reattachment point.

The initial 2D structures found in this study are very similar to those found in plane mixing layer [3, 6, 20] which is not surprising as they are all under the Kelvin–Helmholtz instability mechanism. Further downstream these 2D structures (rollers) get distorted and then become a sort of hairpin vortices which have not been reported in any transitional separated boundary layer flow but only mentioned by Kiya and Sasaki [22] so far in the turbulent separated boundary layer flow. This is quite different from plane mixing layer in that normally a counter-rotating vortex pairs develop when the two-dimensional configuration gets unstable which are known as braids [6]. Further downstream after the mean reattachment point the streaky structures found in the present study are very similar to those found in a turbulent boundary layer.

ACKNOWLEDGEMENTS

The author gratefully acknowledges the support of EPSRC, DERA and Rolls Royce plc who funded this research. Special thanks to Professor P. R. Voke for his advice and support. The computations were carried out on a Cray J932 at Rutherford-Appleton Laboratory, funded by EPSRC.

REFERENCES

1. Townsend AA. *The Structure of Turbulent Shear Flow*. Cambridge University Press: Cambridge, 1956.
2. Corrsin S. Investigation of flow in an axially symmetric heated jet of air. *NACA Adv. Conf. Rep. 3123*, 1943.
3. Hussain AKMF. Coherent structures—reality and myth. *Physics of Fluids* 1983; **26**:2816–2850.
4. Cantwell BJ. Organized motion in turbulent flow. *Annual Review of Fluid Mechanics* 1981; **13**:457–515.
5. Robinson SK. Coherent motion in the turbulent boundary layer. *Annual Review of Fluid Mechanics* 1991; **23**:601–639.
6. Holmes P, Lumley JL, Berkooz G. *Turbulence*, *Coherent Structures*, *Dynamical Systems and Symmetry*. Cambridge University Press: Cambridge, 1996.
7. Paschereit CO, Gutmark E, Weisenstein W. Coherent structures in swirling flows and their role in acoustic combustion control. *Physics of Fluids* 1999; **11**:2667–2678.

8. Jeong J, Hussain F, Schoppa W, Kim J. Coherent structures near the wall in a turbulent channel flow. *Journal of Fluid Mechanics* 1997; **332**:185–214.
9. Nickels TB, Marusic I. On the different contributions of coherent structures to the spectra of a turbulent round jet and a turbulent boundary layer. *Journal of Fluid Mechanics* 2001; **448**:367–385.
10. Gordeyev SV, Thomas FO. Coherent structure in the turbulent planar jet. Part 1. Extraction of proper orthogonal decomposition eigenmodes and their self-similarity. *Journal of Fluid Mechanics* 2000; **414**:145–194.
11. Chainais P, Abry P, Pinton J. Intermittency and coherent structures in a swirling flow: a wavelet analysis of joint pressure and velocity measurements. *Physics of Fluids* 1999; **11**:3524–3529.
12. Sherif ET (Reporter). Discussion of 'the role of coherent structures'. In *Whither Turbulence? Turbulence at the Crossroads*, Lumley JL (ed.). Springer-Verlag: Berlin, 1989; 170–191.
13. Bonnet JP, Delville J. General concepts on structure identification. In *Eddy Structure Identification*, Bonnet JP (ed.). Springer: Berlin, 1996.
14. Lumley JL. The structure of inhomogeneous turbulent flow. In *Atmospheric Turbulence and Radio Wave Propagation*, Yaglom AM, Tatarski VI (eds). Nauka: Moscow, 1967; 166–178.
15. Loeve MM. *Probability Theory*. Van Nostrand: Princeton, NJ, 1955.
16. Cantwell B. Future direction in turbulence research and the role of organized motion. In *Whither Turbulence? Turbulence at the Crossroads*, Lumley JL (ed.). Springer-Verlag: Berlin, 1989; 97–131.
17. Yang ZY, Voke PR. Large-eddy simulation of separated leading-edge flow in general co-ordinates. *International Journal for Numerical Methods in Engineering* 2000; **49**:681–696.
18. Voke PR, Yang ZY, Savill AM. Large-eddy simulation of transition following a leading-edge separation bubble. In *Engineering Turbulence Modelling and Experiment*, vol. 3, Rodi W, Bergeles G (eds). Elsevier: Amsterdam, 1996; 601–610.
19. Coupland J. Private communication, 1994.
20. Roshko A. The plane mixing layer flow visualization results and three-dimensional effects. *Lecture Notes in Physics*, vol. 136, Springer: Berlin, 1981; 208–217.
21. Tafti DK, Vanka SP. A three-dimensional study of flow separation and reattachment on a blunt plate. *Physics of Fluids A* 1991; **3**:2887–2909.
22. Kiya M, Sasaki K. Structure of large-scale vortices and unsteady reverse flow in the reattaching zone of a turbulent separation bubble. *Journal of Fluid Mechanics* 1985; **154**:463–491
23. Na Y, Moin P. Direct numerical simulation of a separated turbulent boundary layer. *Journal of Fluid Mechanics* 1998; **374**:379–405.

